NUMERIČKA PROCENA AERODINAMIČKIH PERFORMANSI ROTORA VETROTURBINE SA VERTIKALNOM OSOM OBRTANJA I KONCENTRATOROM

NUMERICAL EVALUATION OF AERODYNAMIC PERFORMANCES OF VERTICAL-AXIS WIND TURBINE ROTOR WITH FLOW CONCENTRATOR

Jelena SVORCAN[*1], Ognjen PEKOVIĆ[1], TONI IVANOV[1], Miloš VORKAPIĆ[2],
[1] University of Belgrade, Faculty of Mechanical Engineering, Belgrade, Serbia
[2] ICTM – CMT, University of Belgrade Serbia

https://doi.org/10.24094/mkoiee.020.8.1.135

Usled stalnog porasta iskorišćenja energije vetra, interesovanje za male vetroturbine za urbane sredine se takođe širi. Kako ovakve mašine često funkcionišu u nepovoljnim radnim uslovima (Zemljinom graničnom sloju, vrtložnom tragu okolnih objekata, pri maloj i promenljivoj brzini vetra), moguće je instalirati dodatne elemente čija uloga je da lokalno povećaju brzinu kroz rotor i olakšaju pokretanje vetroturbine. Ovaj rad istražuje prednosti dodavanja optimizovanog koncentratora struje vazduha rotoru vetroturbine sa vertikalnom osom obrtanja. Prostorne, nestacionarne simulacije turbulentnog, nestišljivog opstrujavanja izolovanog rotora koji sadrži tri prave lopatice kao i rotora sa koncentratorom izvedene su u softverskom paketu ANSYS FLUENT metodom konačnih zapremina za nekoliko različitih radnih režima. Ova vrsta proračuna je izazovna jer su napadni uglovi visoki, javljaju se brojni strujni fenomeni i nestabilnosti dok interakcija između lopatica i odvojenih vrtloga može biti značajna.Obrtno kretanje lopatica rešeno je pristupom klizajućih mreža. Strujno polje modelovano je nestacionarnim Navije-Stoksovim jednačinama osrednjenim Rejnoldsovom statistikom (URANS) koje su zatvorene k-ω SST turbulentnim modelom. Prikazane su i kvantitativne i kvalitativne analize dobijenih numeričkih rezultata. Naročito je izvršeno poređenje dve krive koeficijenta snage i naglašene su prednosti instaliranja koncentratora struje vazduha.

Ključne reči: *vetroturbina; koncentrator; proračunska aerodinamika; koeficijent snage*

With wind energy extraction constantly increasing, the interest in small-scale urban wind turbines is also expanding. Given that these machines often work in adverse operating conditions (Earth's boundary layer, vortex trails of surrounding objects, small and changeable wind speeds), additional elements that locally augment wind velocity and facilitate turbine start may be installed. This paper investigates possible benefits of adding an optimized flow concentrator to a vertical-axis wind turbine (VAWT) rotor. Three-dimensional, unsteady, turbulent, incompressible flow simulations of both isolated rotor consisting of three straight blades and a rotor with flow concentrator have been performed in ANSYS FLUENT by finite volume method for several different operational regimes. This type of flow simulations is challenging since flow angles are high, numerous flow phenomena and instabilities are present and the interaction between the blades and detached vortices can be significant. The rotational motion of the blades is solved by the unsteady Sliding Mesh (SM) approach. Flow field is modeled by Unsteady Reynolds Averaged Navier-Stokes (URANS) equations with k-ω SST turbulence model used for closure. Both quantitative and qualitative examinations of the obtained numerical results are presented. In particular, the two computed power coefficient curves are compared and the advantages of installing a flow concentrator are accentuated.

Key words: *VAWT; flow concentrator; CFD; power coefficient*

[*] Corresponding author, email: jsvorcan@mas.bg.ac.rs

1 Introduction

The growing and widespread consciousness of the fossil fuels finality in the past few decades has also led to an accelerated development of the techniques for the energy extraction from renewable resources. Apart from solar, wind energy offers the greatest possibilities for technological advancement and economic exploitation [1]. Wind farms have become a common sight all over the world, Serbia included. Although the first thing that comes to mind when talking about wind farms are large-scale structures with horizontal axis of rotation, there is another option. It is also possible to install small-scale vertical-axis wind turbines (VAWTs) in densely populated areas and urban surroundings where winds are weaker and highly changeable in both space and time [2-3].

Main advantages of VAWTs are their low production and maintenance costs, omnidirectional operability in "dirty", slower winds and decreased noise. On the other hand, their efficiency is low compared to horizontal-axis wind turbines (HAWTs), but can be significantly improved by adequate design, installation and control or by addition of outer elements whose purpose is to direct the flow and locally augment the wind speed, and consequently generated power. This paper investigates the possible benefits of the flow concentrator to the aerodynamic performances of a small-scale VAWT.

Here, the two halves of the flow concentrator are shaped like half-ellipsoids whose semi-major a and semi-minor b axes were optimized in one of the previously performed studies with respect to the oncoming undisturbed velocity profile (defined in accordance with the Earth's boundary layer).

In order to accurately estimate aerodynamic performances of VAWTs many computational models have been tried [4-5], ranging from the simplest momentum models to the full Navier-Stokes equations. However, due to the complex, unsteady aerodynamics and numerous flow phenomena that might appear, contemporary approach to resolving the flow around VAWTs usually assumes performing detailed, spatial and transient CFD simulations [6-10]. The performed numerical study is therefore quite challenging due to the non-uniform wind speed, high values of instantaneous angles-of-attack α and significant interaction between the blades and detached wakes.

2 Numerical simulation

Aerodynamic performances of both an isolated and shrouded (by flow concentrator) wind turbine rotor were estimated by finite volume method in the commercial engineering software package ANSYS FLUENT [11]. The following subsections provide details of the adopted computational approach and made assumptions as well as computational choices/compromises.

2.1 Geometric model

The characteristics of the small-scale straight-bladed VAWT rotor used in this computational study and illustrated in Figure 1 are as follows: rotor radius is R = 0.75 m, blade length is L = 1.5 m, number of blades is N_b = 3, blade chord is c = 0.10 m resulting in rotor solidity $\sigma = (N_b c)/(2R) = 0.2$. This lower solidity value generally provides greater values of maximal power coefficient. In order to decrease the rotor production costs, blades are straight and untwisted with the cross-section shaped like a NACA 0018 airfoil.

Flow concentrator comprises two parts, lower and upper half-ellipsoids defined by the values of its semi-major and semi-minor axis. Geometric parameters of the lower part are a_2 = 2.2 m and b_2 = 0.97 m, and of the upper part are a_1 = 1.92 m and b_1 = 1.0 m. These values were obtained after an optimization study that was performed for a power-law velocity profile assumed along the inlet boundary:

$$V(h) = V_o \left(\frac{h}{h_o} \right)^{\alpha} . \tag{1}$$

For the sake of comparison and validation of the performed shape optimization study, an arbitrary flow concentrator geometry was also numerically investigated. This was done in order to observe the differences between the flow fields that appear around an optimized and ordinary concentrator geometry.

The rotational zone of the computational domain is shaped like a hollow cylinder encircling the three blades. Its inner and outer diameters are $d = 1.25$ m and $D = 1.75$ m, respectively. It is also depicted in Figure 1. In order to make the grid generation possible, its height is slightly bigger than the length of the blades.

The extents of the outer stationary sub-domain are: $-5a$ fore and $12a$ aft the central wind turbine shaft along the longitudinal x-axis, $\pm 5a$ along the lateral y-axis and $5L$ along the vertical z-axis starting from the ground where $z = 0$ m.

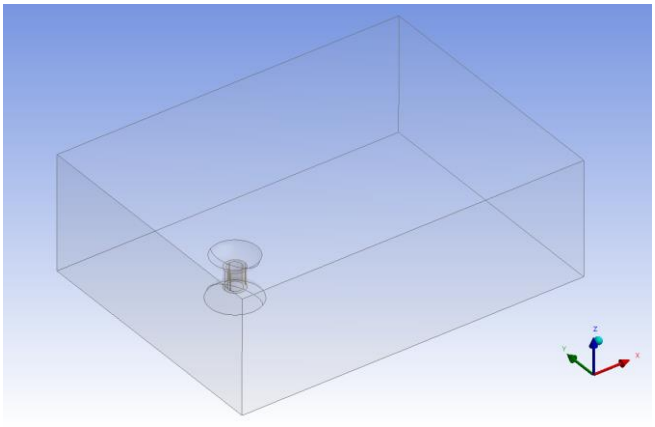

Figure 1. Computational domain with boundaries and separate zones, VAWT rotor and flow concentrator

2.2 Computational grid

Hybrid unstructured computational meshes containing approximately 3-3.2 million cells were used in computations. These medium fine grids were adopted as a compromise between the significant computational complexity on one hand, and limited computational recourses on the other.

Global size functions are applied across the computational domain. They are used to refine the interface surfaces (face sizing 2.5 cm) and ensure that small edges and surfaces are represented correctly (proximity & curvature option). Size functions are also defined along the blade edges, in the chord- and span-wise directions (number of elements is 50 and 60, respectively, while the ratio of the biggest-to-smallest edge size is 5), enabling the creation of the structured mesh along the blade upper and lower surfaces. Cells grow larger in the radial direction from the central shaft towards the outer boundaries.

For modeling the flow adjacent to blade walls as the most critical (in the rotational part of the computational domain), $N = 25$ layers of prismatic cells with a growth rate $q = 1.2$ and the first layer thickness $y_1 = 0.07$ mm resulting in dimensionless distance from the wall $y^+ < 5$ were created. Boundary layers were somewhat relaxed around the flow concentrator ($N = 20$, $q = 1.2$, $y_1 = 0.5$ mm) and ground ($N = 30$, $q = 1.2$, $y_1 = 1.0$ mm) surfaces in order to reduce the total number of elements. Figure 2 provides a detail of one of the used computational meshes.

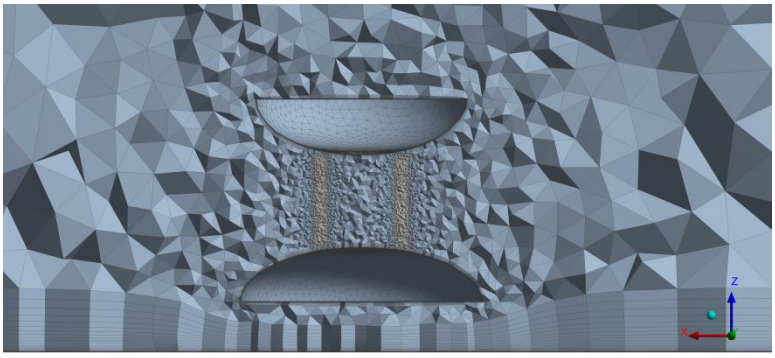

Figure 2. Detail of the used computational grid

2.3 Zonal and boundary conditions

Fluid flow around the wind turbine rotor with and without the flow concentrator is modeled as unsteady and viscous (turbulent). Due to the small velocities, fluid, air, was considered as incompressible gas of constant dynamic viscosity.

The following boundary conditions are defined. At the "velocity inlet" the height-varying magnitude and direction of the undisturbed wind speed V_o together with turbulent quantities − intensity t = 5% and relative turbulent viscosity ν_t/ν = 10 are assumed. At the "pressure outlet" the constant value of gauge pressure is set Δp = 0 Pa. Blades are considered as no-slip rotational walls, while the concentrator walls are stationary.

In order to accomplish different values of tip-speed ratio $\lambda = R\Omega/V_o$ at constant undisturbed wind speed, the rotational motion of the inner zone with angular velocity Ω varied is modeled by the "sliding mesh" approach where the nodes and cells of the rotor mesh zone perform a rigid body rotational motion relative to the outer stationary zone [11]. The interpolation of flow quantities is performed along a non-conformal interface surface separating the two sub-domains.

2.4 Numerical set-up and schemes

Unsteady Reynolds-averaged Navier-Stokes equations are closed by a two-equation k-ω SST turbulence model, based on Boussinesq hypothesis, that presents a combination of standard k-ω model near the walls and k-ε in the outer layer. Its features (modifications) make it more accurate and reliable for flows including airfoils, adverse pressure gradient flows, etc. [12].

Since the flow is considered as incompressible, pressure-based solver is employed, with SIMPLEC pressure-velocity coupling scheme. All spatial derivatives are approximated by 2nd order schemes, while the temporal discretization is of the 1st order.

Time step, dt = T/180, corresponds to $\Delta\theta$ = 2° angular increment. Ten iterations per time-step were performed. Simulations for each working regime lasted 3-5 revolutions until reaching quasi-convergence of aerodynamic moment coefficients.

3 Results and discussion

3.1 Quantitative analysis

During each simulation, the values of instantaneous torque Q around the rotation axis are registered. Figure 3 illustrates the computed fluctuations of the torque throughout a single rotation at tip-speed ratio λ = 3.5 for all three investigated geometries. The highest values obtained with the optimal flow concentrator are marked by a solid black line.

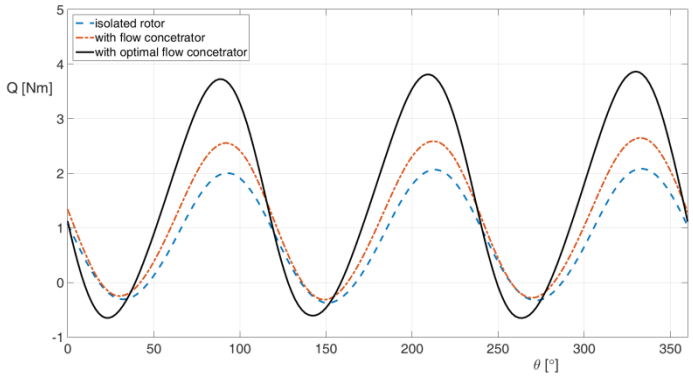

Figure 3. Torque curves during rotor rotation at λ = 3.5

Mean rotor power P can then be computed as the product of total shaft torque averaged per rotation Q_{mean} and its angular velocity Ω. Power coefficient presents the portion of attainable wind energy. It is estimated as:

$$C_P = \frac{P}{0.5\rho V_o^3 A}. \tag{2}$$

Computed power coefficient curves $C_P(\lambda)$ of all three considered geometries are presented in Figure 4.

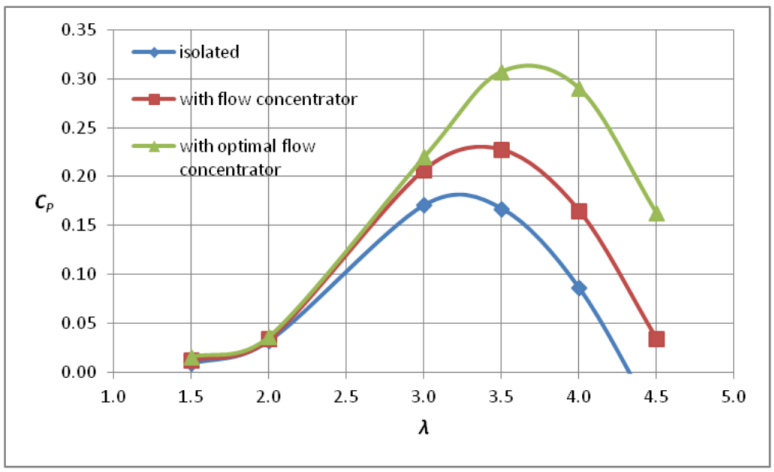

Figure 4. Computed power coefficient curves $C_P(\lambda)$

Figure 4 demonstrates several important facts: wind turbine rotor can be started at low wind speeds, $\lambda_{min} \approx 1.0$, both without and with the flow concentrator, i.e. the addition of flow concentrator to the rotor does not reduce the starting qualities of small-scale VAWTs, and the maximal expected power coefficient of an isolated rotor of $C_{P,max} \approx 0.17$ achieved at optimal working regime $\lambda_{opt} \approx 3.1$ can be increased to $C_{P,max} \approx 0.31$, i.e. more than 80%, achieved at $\lambda_{opt} \approx 3.5$ with the optimized geometry of the flow concentrator. This significant increase of both the power coefficient C_P and extracted power P is primarily due to two circumstances: *i*) the accelerated flow field through the flow concentrator, i.e. the increase in available wind power, but also *ii*) more efficient deceleration through the rotor shrouded by the flow concentrator which is precisely what a wind turbine rotor should do − slow down the oncoming air flow and turn the extracted kinetic energy of translational motion to rotational. The changes of velocity profiles across the isolated rotor and the rotor shrouded by the optimal flow concentrator are depicted in Figure 5. The presented values of x-coordinate are measured with respect to the rotational axis where $x = 0$ m, while $x = -0.75$ m and $x = 0.75$ m lie fore and aft of the axis.

a)

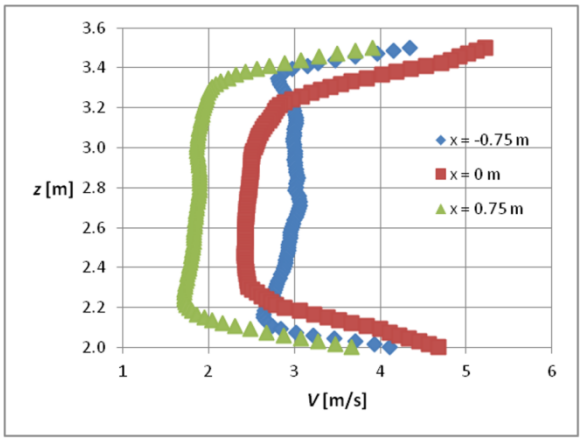

b)

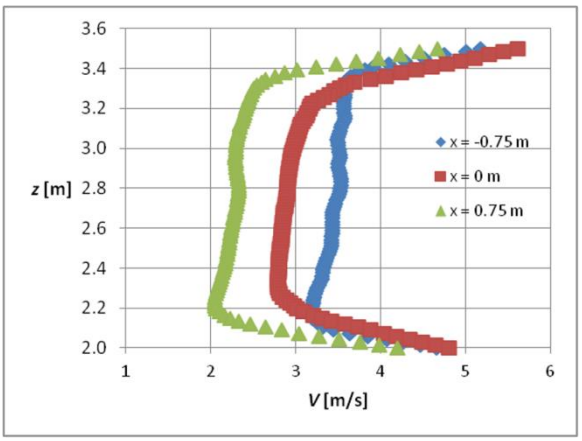

Figure 5. Computed velocity profiles for: a) the isolated rotor and b) the rotor with the optimal flow concentrator

3.2 Qualitative analysis

Finally, instantaneous flow visualizations in the shape of velocity contours and streamlines, respectively, are depicted in Figures 6-7 for $\lambda = 3.5$ and the two rotors, without and with optimal flow concentrator. The effects of both the rotor and flow concentrator on the oncoming air stream are apparent through decelerated zones marked in the dark shades of blue.

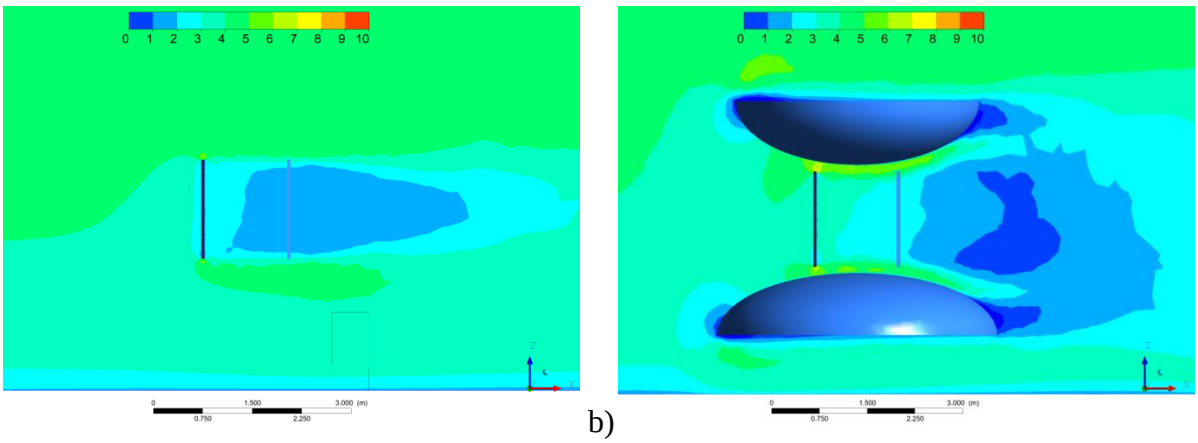

a) b)

Figure 6. Computed velocity contours around: a) an isolated rotor and b) a rotor with optimal flow concentrator

Apart from locally augmenting the wind speed by making the streamlines through the rotor more compact, the flow concentrator enables the increased deceleration of wind speed by greater expansion of the streamlines downstream of the rotor, i.e. increased energy extraction resulting in higher values of power coefficient. Its benefits are numerous and can be further optimized for a particular location by a proper definition of its geometric parameters.

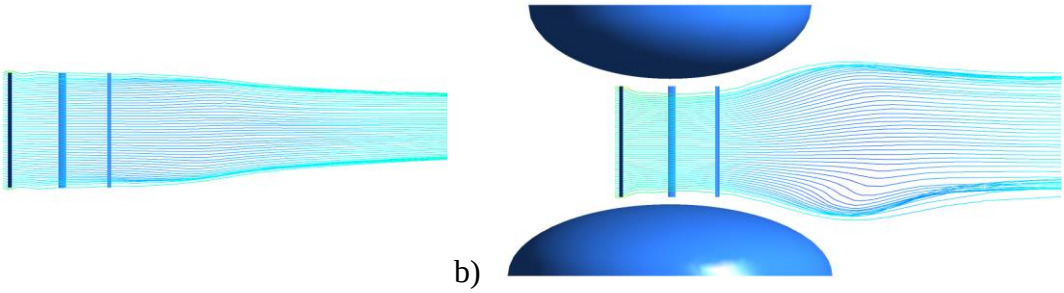

a) b)

Figure 7. Computed streamlines around: a) an isolated rotor and b) a rotor with optimal flow concentrator

4 Conclusions

The most important conclusions from the performed study can be summed up as follows.

The paper provides a detailed description of all the necessary steps for performing numerical simulation of the 3D, unsteady fluid flow around a vertical-axis wind turbine rotor.

It also investigates the means to improve VAWT efficiency in urban environments by adding additional elements.

By installing a flow concentrator of optimal geometry for a particular location and wind speed profile, the estimated efficiency improvement amounts to more than 80% at tip-speed ratios close to optimal.

Future work will include a more detailed study of the flow concentrator on high-solidity VAWT rotors where the interference between the blades and the shed wakes is more significant.

5 Acknowledgement

This research work was supported by the Ministry of Education, Science, and Technological Development of Republic of Serbia through contracts no. 451-03-68/2020-14/200105 and 451-03-68/2020-14/200026.

6 References

[1] ***, **IR**ENA, Renewable capacity statistics 2019, International Renewable Energy Agency (IRENA), Abu Dhabi, UAE, 2019.

[2] Bhutta, M. M. A., N. Hayat, A. U. Farooq, Z. Ali, Sh. R., Jamil, Z. Hussain, Vertical axis wind turbine – A review of various configurations and design techniques, Renewable and Sustainable Energy Reviews, 16(2012), 4, pp. 1926–1939.
[3] Stathopoulos, T., H. Alrawashdeh, A. Al-Quraan, B. Blocken, A. Dilimulati, M. Paraschivoiu, P. Pilay, Urban wind energy: Some views on potential and challenges, Journal of Wind Engineering and Industrial Aerodynamics, 179(2018), pp. 146–157.
[4] Islam, M., D. S. -K. Ting, A. Fartaj, Aerodynamic models for Darrieus-type straight-bladed vertical axis wind turbines, Renewable and Sustainable Energy Reviews, 12(2008), 4, pp. 1087–1109.
[5] Manwell, J. F., J. G. McGowan, A. L. Rogers, Wind energy explained, Theory, Design and Application, 2nd edn, John Wiley & Sons Ltd., Chichester, UK, 2009.
[6] Howell, R., N. Qin, J. Edwards, N. Durrani, Wind tunnel and numerical study of a small vertical axis wind turbine, Renewable Energy, 35(2010), pp. 412–422.
[7] Nini, M., V. Motta, G. Bindolino, A. Guardone, Three-dimensional simulation of a complete Vertical Axis Wind Turbine using overlapping grids, Journal of Computational and Applied Mathematics, 270(2014), pp. 78–87.
[8] Balduzzi, F., J. Drofelnik, A. Bianchini, G. Ferrara, L. Ferrari, M. S. Campobasso, Darrieus wind turbine blade unsteady aerodynamics: a three-dimensional Navier-Stokes CFD assessment, Energy, 128(2017), pp. 550–563.
[9] Franchina, N., G. Persico, M. Savini, 2D-3D Computations of a Vertical Axis Wind Turbine Flow Field: Modeling Issues and Physical Interpretations, Renewable Energy, 136(2019), pp. 1170–1189.
[10] Guillaud, N., G. Balarac, E. Goncalves, J. Zanette, Large Eddy Simulations on Vertical Axis Hydrokinetic Turbines − Power coefficient analysis for various solidities, Renewable Energy, 147(2020), pp. 473–486.
[11] ***, ANSYS Fluent Theory Guide, Release 16.0, ANSYS, Inc., Canonsburg, USA, 2015.
[12] Menter, F. R., M. Kuntz, R. Langtry, Ten Years of Industrial Experience with the SST Turbulence Model, In: Proceedings of the 4th International Symposium on Turbulence, Heat and Mass Transfer, pp. 625–632, Begell House Inc., West Redding, USA, 2003.